

LBL--27894

LBL - 27894

DE90 003082

BINARY COMPLEX FRAGMENT EMISSION AND MULTIFRAGMENTATION
FROM VERY HOT NUCLEI

L. G. MORETTO AND G. J. WOZNIAK
Lawrence Berkeley Laboratory, 1 Cyclotron Road,
Berkeley, California 94720, USA

International School Seminar on Heavy Ion Physics,
Joint Institute for Nuclear Research, Dubna, Russia, October 3-12, 1989

This work was supported by the Director, Office of Energy Research,
Division of Nuclear Physics of the Office of High Energy and Nuclear Physics
of the U.S. Department of Energy under Contract DE-AC03-76SF00098.

DISTRIBUTION OF THIS DOCUMENT IS UNLIMITED

OK
10/10/89

BINARY COMPLEX FRAGMENT EMISSION AND MULTIFRAGMENTATION FROM VERY HOT NUCLEI

L. G. Moretto and G. J. Wozniak

Nuclear Science Division, Lawrence Berkeley Laboratory
1 Cyclotron Rd, Berkeley, CA 94720, USA

Abstract: Complex fragments at low and intermediate energies originate mostly from the binary decay of a compound nucleus formed in either complete or incomplete fusion. With increasing bombarding energy incomplete fusion should terminate. Evidence of this occurrence is given. As the excitation energy increases, multifragment decay becomes prevalent. The sources of ternary and quaternary events, characterized in terms of their velocity and total charge, do not seem to differ from that of binary events.

Introduction

Intermediate energy heavy-ion reactions have led to the formation of extremely hot nuclei, very near the expected limit of their stability. A great deal of the work in this field has been dedicated to their characterization, either through their massive neutron emission,^{1/} or through their production of complex fragments.^{2/} Simultaneously, the reaction mechanism leading to the formation of these nuclei has been the subject of intense study.

Complex fragment production provides information about both aspects of the problem. On the one hand, complex fragments have been shown to be emitted in the decay of hot, relatively long-lived sources, which frequently can be identified with compound nuclei originating from complete or incomplete fusion.^{2/} On the other hand, they also appear to be associated with the target- or projectile-like remnants arising in either deep inelastic reactions or incomplete fusion reactions. Thus, the study of complex fragments plays an essential role in the characterization of the very hottest nuclei, as well as of the process of their formation.

The Demise of Incomplete Fusion and the Onset of the Fireball Regime.

At bombarding energies below 10 MeV/A, the dominant reaction mechanisms are deep inelastic reactions on the one hand, and complete fusion on the other. For very mass asymmetric entrance channels, the complete fusion process seems to continue up to bombarding energies as high as 18 - 20 MeV/A.^{3/} The study of these complete fusion products through their complex fragment decay shows very sharp sources with velocities typical of complete fusion.

The demise of complete fusion and the onset of incomplete fusion can be observed in two ways: by decreasing the mass asymmetry of the entrance channel, and/or by increasing the bombarding energy. The first way is illustrated in Fig. 1. In this figure three reactions are considered. The 18 A MeV ^{139}La projectile is the same, while the three targets are ^{12}C , ^{27}Al and ^{64}Ni . Thus, all three reactions are observed in reverse kinematics. The energy-relaxed binary decays are studied and the events' centers-of-mass velocities are shown. In the case of the ^{12}C and ^{27}Al targets, sharp sources corresponding to complete fusion are observed. The widths of these velocity distributions are attributed to light particle decays either preceding or following the binary process. In the case of the ^{64}Ni target, one observes a well defined

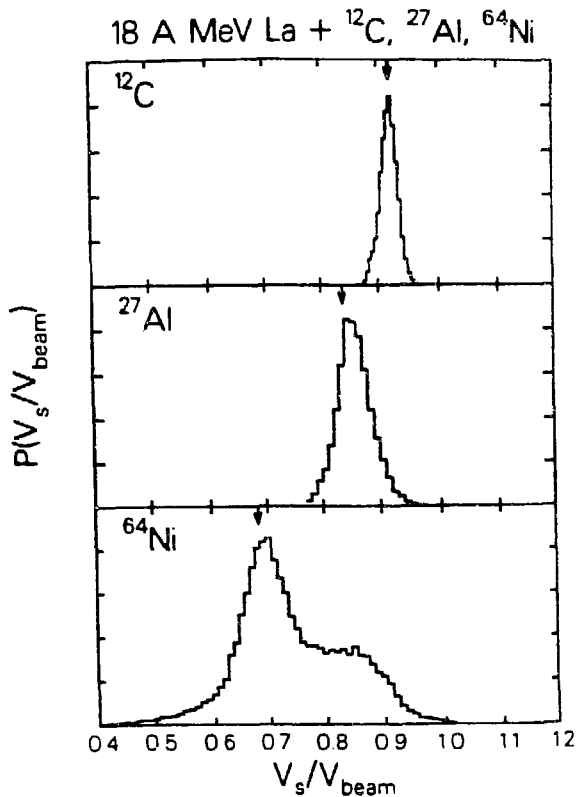


Fig. 1 Source velocity distributions for the 18 A MeV $^{139}\text{La} + ^{12}\text{C}$, ^{27}Al , ^{64}Ni reactions as extracted from the binary coincidences. The vertical arrows indicate the velocities corresponding to complete fusion for the three reactions.¹⁴

complete fusion peak (corresponding to ~ 800 MeV of excitation energy!), but also a tail at higher velocities indicating that the binary decay does arise from an incomplete fusion of the ^{64}Ni target with the La projectile.¹⁴

If the entrance channel system is very asymmetric, an increase in bombarding energy still reveals rather sharp sources in the complex fragment decay. However, these sources do not have a velocity corresponding to complete fusion; rather their velocity is consistent with incomplete fusion of the smaller nucleus with the larger. This is illustrated in Fig. 2, where a very asymmetric reaction at two different bombarding energies is considered.¹⁵ One observes that sharp sources of binary decays are still produced. These velocities are essentially independent of the exit channel mass asymmetry, but indicate that only part of the target fuses with the projectile. The sharpness of the sources visible in these experiments may well be accentuated by the requirement of sufficient excitation energy to produce complex fragments with reasonable probability. Hence, small mass transfers should be almost invisible because the resulting small excitation energy does not favor compound nucleus emission of complex fragments.

In a vivid and possibly correct picture of incomplete fusion, the heavy nucleus cuts through the light nucleus, incorporates the overlapping part, and leaves behind a light remnant as a spectator. The object

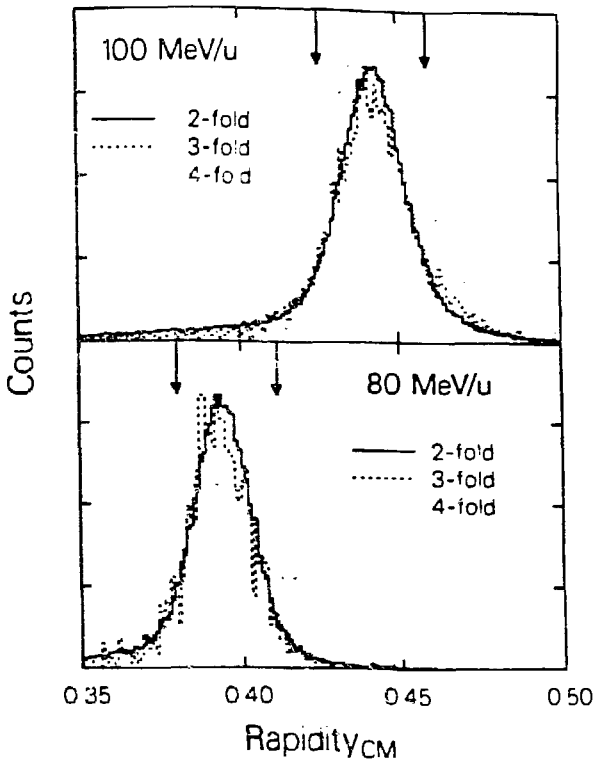


Fig. 2 Distributions of the center-of-mass rapidity for 2-fold, 3-fold, and 4-fold complex fragment ($Z > 2$) events in the 80 and 100 MeV/u $^{139}\text{La} + ^{12}\text{C}$ reactions. The maxima of the distributions have been normalized to each other. The arrow at larger rapidity in each subplot indicates the beam rapidity. The arrow at smaller rapidity indicates the center-of-mass rapidity of the entrance channel.¹⁵

formed in this incomplete fusion process proceeds to relax into a compound nucleus, and to decay accordingly. If the cutting of one nucleus into the other proceeds along the geometrical edge of the heavy nucleus, and if the only relevant energy in the process is that associated with the extra surface created in the cutting, it is easy to calculate the threshold for incomplete fusion for any given impact parameter, as well as the velocities of both fused product and light spectator after the reaction.^{16/} A large amount of survey work at energies near the onset of incomplete fusion has been produced, although no truly systematic study characterizing the threshold as a function of impact parameter has been undertaken as yet.

This model predicts, in general, a broad range of incomplete fusion products (sources), due to the range of impact parameters accessible to the reaction. The apparent contradiction with the relatively sharp complex fragment sources observed in very asymmetric systems is now understood as caused by the invisibility of the small excitation energy-small angular momentum sources associated with the largest impact parameters. However, as we have seen before, the use of more symmetric target-projectile combinations does in fact reveal a broad range of complex fragment sources with a continuum of velocities, mass transfers and excitations energies, extending to the complete fusion limit. In this study, the coincident detection of the source binary-decay products has been essential in characterizing the mass, energy and momentum transfer of the reaction.

As the bombarding increases to very large values, we can imagine that, as the lighter nucleus is cut by the impact of the heavier nucleus, the heavier nucleus will also be cut by the impact of the lighter nucleus.

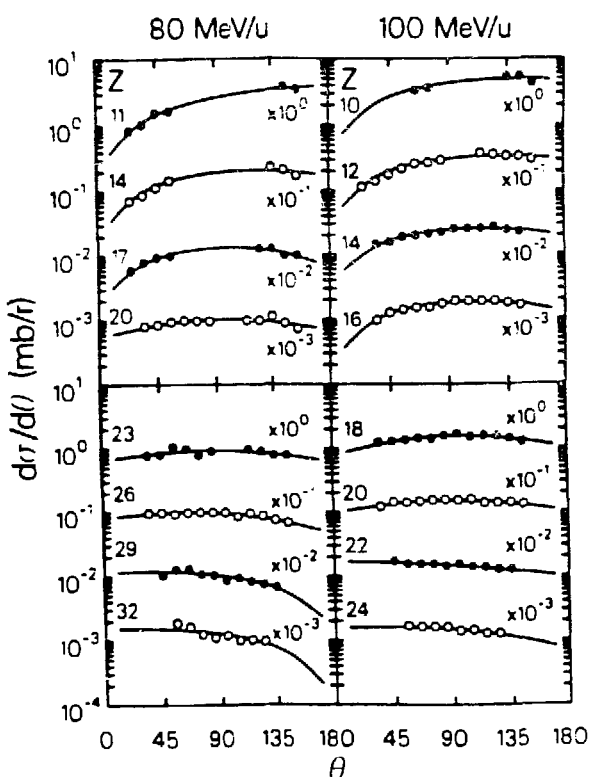


Fig. 3 Angular distributions in the c.m. system for representative Z-values from the 80 & 100 MeV/u $^{139}\text{La} + ^{12}\text{C}$ reactions.^{15/}

This should occur when the inertial forces overcome the forces necessary to produce each of the cuts. In this situation, incomplete fusion should cease, since neither partner will be able to resist the impact of the overlapping part of the other nucleus and to absorb it. Thus, three pieces are expected: the two relatively cold spectators which are the remnants of the original partners, and the hot object formed by the fusion of the two overlapping regions (fireball).

While there is some good evidence for this fireball regime at very high bombarding energies, the transition region corresponding to the demise of incomplete fusion and to the onset of the fireball regime has not been characterized at all. We do not know if this transition is sharp or smooth, nor at which bombarding energy it should occur. This is certainly one of the most important landmarks in the landscape of intermediate energy heavy ion reactions, that should be eminently accessible by studying the complex fragments produced in the reaction.

At what energy will this decoupling of the fireball from the heavy reaction partner occur? An estimate from an incomplete fusion model for the reaction $^{139}\text{La} + ^{12}\text{C}$ suggests that the decoupling ought to occur around 80 A MeV./5.6/

Indeed dramatic changes and novel features have been observed in the reaction $^{139}\text{La} + ^{12}\text{C}$ at 80 & 100 A MeV that may be related to the incipient decoupling of the fireball. In this reaction the appearance of well defined Coulomb rings at all atomic numbers indicates the presence of a fairly sharp source and the predominance of binary decay. However, the distributions along the Coulomb rings are not isotropic. They are backward peaked from $6 \leq Z \leq 18$, side peaked from $19 \leq Z \leq 25$ and forward peaked for $Z > 26$, the rather broad peak moving continuously from one extreme to the other as shown in Fig. 3. This behavior is quite new. For instance, in the same reaction at 18 A MeV, the backward peaking is confined $Z < 8$ and the forward peaking to $Z > 40$, while a rigorously flat distribution is observed for all of the intermediate Z -values. At 50 A MeV, the products of $22 \leq Z \leq 35$ are still forward/backward symmetric. The perturbation in the angular distributions observed at higher energies seems to be dynamical in origin. It is possible that the nascent fireball, still attached to the heavy partner tries to detach itself by stretching out toward the light partner spectator. The decay may then occur from this stretched configuration giving rise to a rather light fragment pointing toward the backward hemisphere where the light spectator is

located. At much larger energies, where the decoupling of the fireball is complete and the fragments are emitted from the target spectator, the angular distributions are very nearly isotropic.

The total cross sections as a function of atomic number shown in Fig. 4 are also rather peculiar. The Z distribution is U shaped and shows no hint of a symmetric peak, while at lower energies the symmetric peak is most prominent. Of course an increase in temperature is expected to flatten out the distribution and to reduce the sharpness of the symmetric peak. However, here the central peak is totally absent and the cross section increases dramatically for $Z < 20$. This distribution may indicate the presence of dynamical effects. In particular, the fragments with $Z < 20$ may very well be associated with the breaking off of the stretched out portion of the system associated with the nascent fireball.

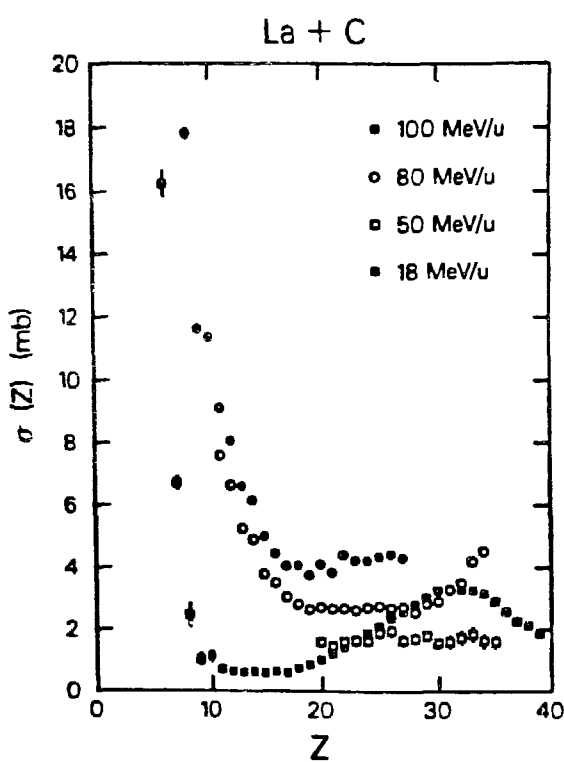


Fig. 4 Angle-integrated cross sections of products from the 18, 50, 80 and 100 MeV/u $^{139}\text{La} + ^{12}\text{C}$ reactions. The bars of some of the points are the statistical errors; where bars do not appear the errors are smaller than the size of the data points.

Complex Fragments and the Decay of Hot Nuclei.

Much has been theorized about the limits of stability of very hot nuclei. The existence of a critical temperature above which the liquid and the vapor phases of the nuclear fluid lose their identity has been postulated on the basis of the standard theory of classical fluids.^{2/} The fact that nuclei are at best tiny drops of this fluid, and are affected very much by long range forces, like the Coulomb force, may change the picture drastically, both quantitatively (e.g. regarding the exact value of the critical temperatures) and qualitatively (e.g. regarding the existence or not of a relatively sharp second-order transition).

Furthermore, should the loss of stability turn out to be of the nature described above, it is not clear how this instability should manifest itself, especially in view of the fact that nucleonic and complex fragment emission does occur already well below the expected onset of this instability. The evidence available at present indicates that extended, highly thermalized sources are produced in most collisions. Neutron

multiplicities and temperature determinations lead to the confirmation of excitation energies as high as 4-5 MeV/A. Long lived intermediate systems have been characterized in terms of their mass, charge, excitation energy and to a more limited extent, angular momentum from their binary decay into complex fragments. In many instances it turns out that this complex fragment emission follows the statistical branching ratios expected for compound nucleus decay. This makes these intermediate systems honest-to-goodness compound nuclei, with excitation energies quite near the expected maximum.^{2/3/} On the other hand the observation of compound nucleus emission of complex fragments at low energy^{7,8/} implies that abundant emission at higher energies is to be expected.

Part of the initial confusion about complex fragment emission at intermediate energies may have been due to the broad range of compound and non compound nucleus sources associated with the onset and establishment of incomplete fusion. This problem can be minimized to some extent by the choice of rather asymmetric systems. In such systems, the range of impact parameters is geometrically limited by the nuclear sizes of the reaction partners. Furthermore, the projectile-like spectator, if any, is confined to very small masses, and does not obscure other sources of complex fragments. Many reactions have been studied in

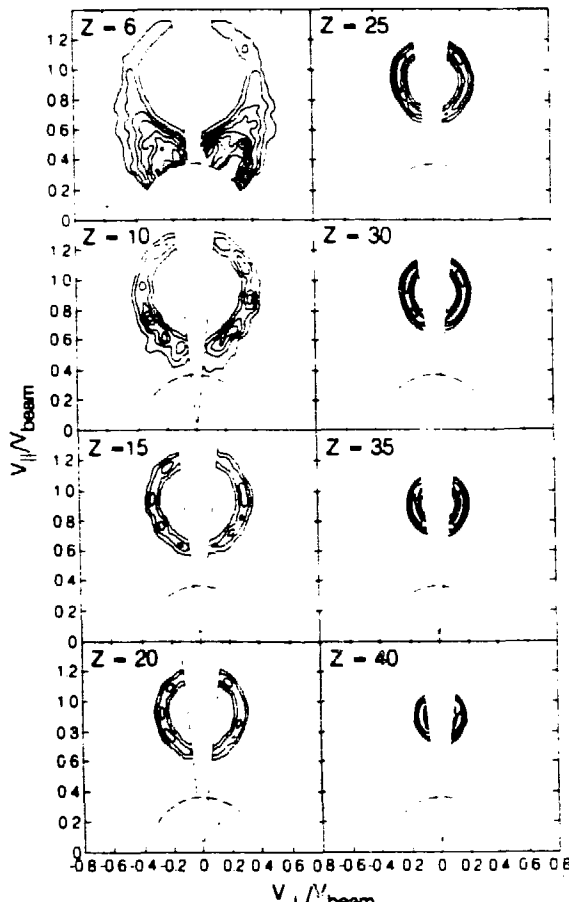


Fig. 5 Contours of the experimental cross section $\partial^2\sigma/\partial V_{\parallel}\partial V_{\perp}$ in the $V_{\parallel} - V_{\perp}$ plane for representative fragments detected in the reaction $E/A = 18 \text{ MeV } ^{139}\text{La} + ^{12}\text{C}$. The beam direction is vertical towards the top of the figure. The dashed lines show the maximum and minimum angular thresholds and the low velocity threshold of the detectors. The magnitudes of the contour levels indicated are relative.^{9/}

Table 3.1. Annealing performance measures for templates 1 through 6.

Templates	1	2	3	4	5	6
Inclination set 1	0	30	37.5	45	0	45
Inclination set 2	60	90	97.5	90	90	135
Inclination set 3	120	150	157.5	157.3	-	-
Number of iterations until convergence	1370	1410	1441	1277	1315	1264
Minimum energy	4.0 e^{-3}	1.01 e^{-5}	17.6 e^{-5}	11 e^{-5}	5.7 e^{-5}	5.8 e^{-5}

The energies are all low enough to give negligible mean squared error. The energy is the sum of the squared difference between the "real" head values at the wells and the values of the wells in the annealing solution. The "real" steady state head values range from zero to one. We consider any head difference less than 0.01 to be effectively zero, and all the energies are below 0.005. The average head difference for each well is therefore under 0.01.

Based on this limited sample we believe that the geologic information incorporated into the template for the MI site will improve the solution.

3.3. Effect of the Starting Point

Many different configurations of channels can equally well match the hydrologic data available at a site. We are interested in obtaining a range of flow geometries. However, we expect that the flow geometries should have approximately the same density of channels in order to have the same connectivity.

One might believe that the set of configurations which match the hydrological data can be grouped or categorized. For example, some solutions may tend to have a "hole" in a certain location and others in a different location. These groups may each be associated with a different valley in the energy function. One might be able to reach a certain valley starting from some initial points but not others. One way to find flow geometries in these different valleys might be to start from widely separated configurations and different random seeds. The beginning configurations could also have different percentages of "on" pipes. If we can start from points

Nb + Be

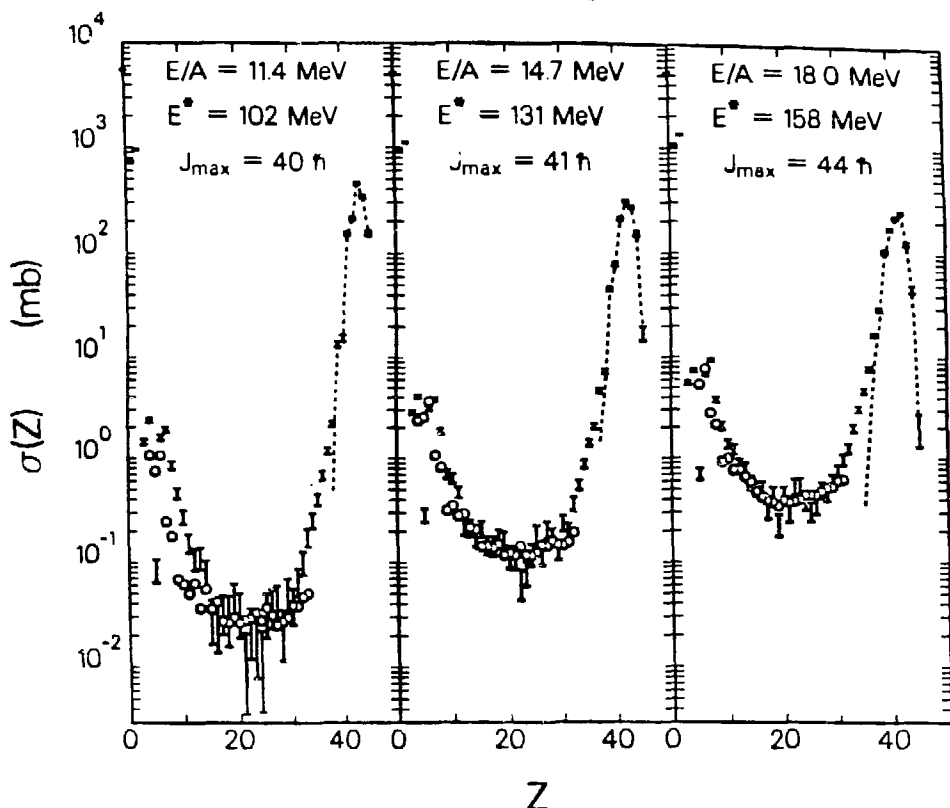


Fig. 7 Comparison of experimental and calculated charge distributions for the $^{93}\text{Nb} + ^9\text{Be}$ reaction at $E/A = 11.4, 14.7$ and 18.0 . The experimental data are indicated by the hollow circles and the values calculated with the code GEMINI are shown by the error bars. The dashed curve indicates the cross sections associated with classical evaporation residues which decay only by the emission of light particles ($Z \leq 2$). Note the value of the excitation energy (E^*) corresponding to complete fusion and the value of J_{\max} assumed to fit the data.^{3/}

The most important information associated with these cross sections is their absolute value and energy dependence. Through them, the competition of complex fragment emission with the major decay channels, like n , p , and α decay is manifested. This is why we attribute a great deal of significance to the ability to fit such data. Examples of these fits are shown in Figs. 6 & 7. The calculations are performed with an evaporation code GEMINI^{3/} extended to incorporate complex fragment emission. Angular momentum dependent finite-range barriers are used. All the fragments produced are allowed to decay in turn both by light particle emission or by complex fragment emission. In this way higher chance emission, as well as sequential binary emission, are accounted for.^{3/9/} The cross section is integrated over ℓ waves up to a maximum value that provides the best fit to the experimental charge distributions. In the case of the $^{93}\text{Nb} + ^9\text{Be}$ & ^{12}C , as well $^{139}\text{La} + ^{12}\text{C}$ for bombarding energies up to 18 MeV/u, the quality of the fits is exceptionally good and the fitted values of ℓ_{\max} correspond very closely to those predicted by the Bass model or by the extra push model, as shown in Fig. 8.^{3/}

Nb + Be

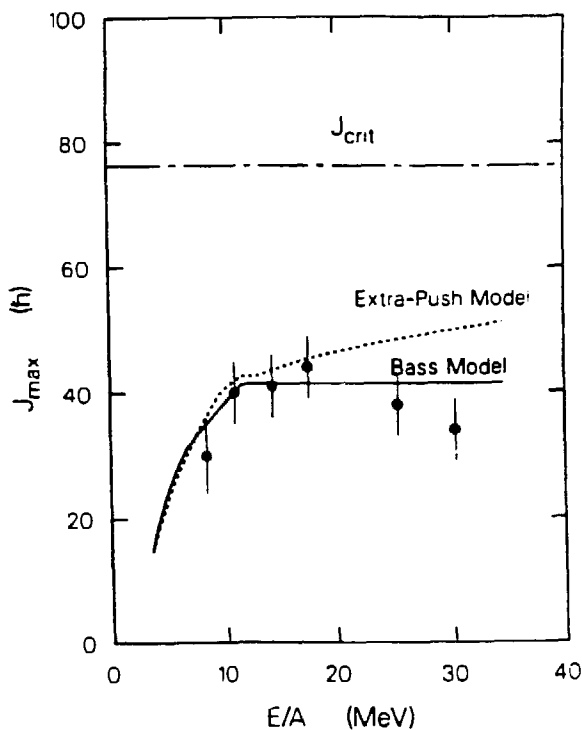


Fig. 8 Plot showing the maximum angular momentum for fusion (J_{\max}) obtained by fitting the experimental charge distributions as a function of bombarding energy for the $^{93}\text{Nb} + ^9\text{Be}$ reactions. The dashed and solid curve show the predictions of the extra-push and Bass models, respectively. The chain dashed lines indicate the angular momentum (J_{crit}) where the barrier for symmetric division vanishes.¹³

bombarding energies are shown in Fig. 9. The corresponding sum ($Z_1 + Z_2$) spectra are also shown in Fig. 10. The binary nature is proven by the correlation angles as well as by the sum of the fragments' atomic numbers which accounts for most of the target + projectile charge. The missing charge can be accounted for by the extent of incomplete fusion and by the sequential evaporation of light charged particles ($A \leq 4$).

The same studies have shown also that the very hot intermediates (compound nuclei) that undergo binary decay into complex fragments, also undergo ternary and quaternary decays into smaller complex fragments.¹⁵ The demise of binary decay in favor of higher multiplicity complex fragment emission can be seen in Fig. 9 where Z_1 vs Z_2 diagrams are shown up to 100 A MeV bombarding energy. The strong diagonal band characteristic of binary decay broadens and becomes accompanied by additional patterns. Similarly, the $Z_1 + Z_2$ spectra become broadened and the peak moves to lower values, as shown in Fig. 10.

La + C

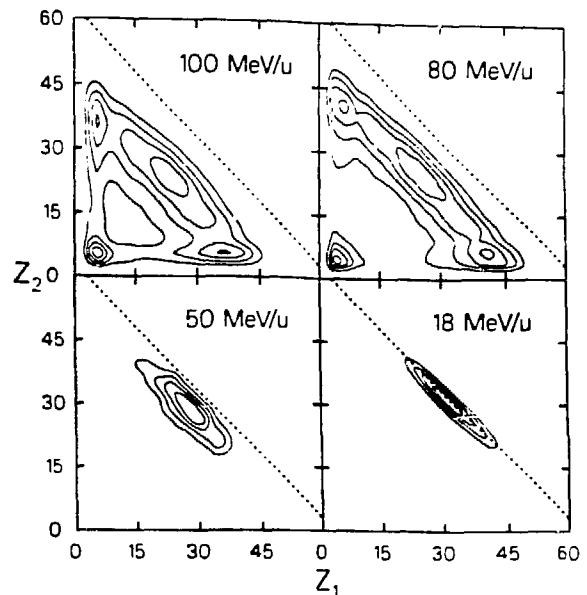


Fig. 9 Representative Z_1 - Z_2 contour plots for coincidence events from the reaction $^{139}\text{La} + ^{12}\text{C}$ at 18, 50, 80 and 100 MeV/u. Z_1 and Z_2 refer to the Z-values of fragments detected in two detectors at equal angles on opposite sides of the beam.¹⁵

If any doubt still remains concerning the binary nature of the decay involved in complex fragment production, it can be removed by the detection of binary coincidences. Several examples of Z_1 - Z_2 correlations observed over a great range of

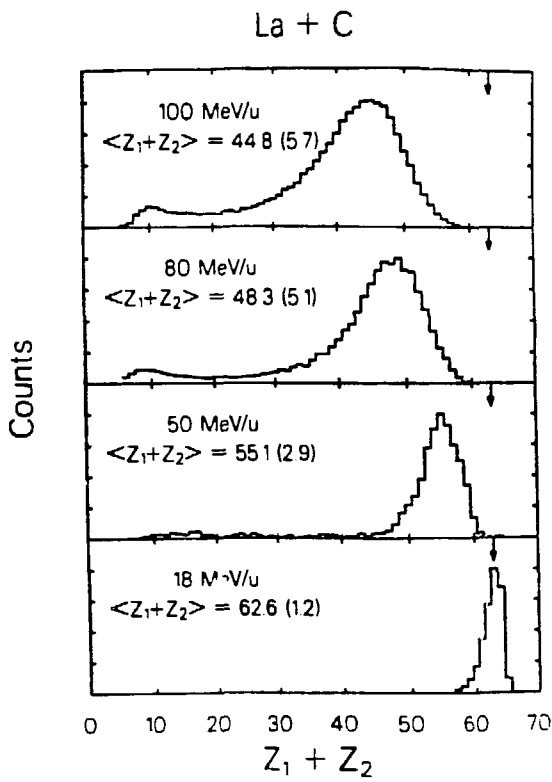


Fig. 10 The relative yield of coincidence events plotted as a function of the sum of the atomic charges of the two coincident fragments for the $^{139}\text{La} + ^{12}\text{C}$ reaction at 18, 50, 80 & 100 MeV/u.^{15/}

The study of binary, ternary and quaternary coincidences is also very instructive. The center-of-mass rapidities extracted for all classes of events are shown in Fig. 2 & 11. The distributions are essentially identical for all multiplicities. This identity suggests that both binary and ternary events arise from the same source. This is made even more likely by the spectra of the total charge for both binary and ternary events at two bombarding energies shown Fig. 12. The identity of these two distributions is striking and in conjunction with the identity of center-of-mass rapidities leaves little doubt on the uniqueness of the source.

The charge distribution of ternary events can be best appreciated by means of a Dalitz plot. In Fig. 13 the plot for ternary coincidences is shown. It has been obtained by gating on the peak of the sum charge distribution, $45 \leq Z_{\text{total}} < 55$, and by plotting Z_1/Z_{total} vs. Z_2/Z_{total} vs. Z_3/Z_{total} . (In a triangular Dalitz plot one would require $Z_1 + Z_2 + Z_3 = \text{constant}$). The band of high cross section along the edges of the triangle means that one of the three fragments is always relatively small.

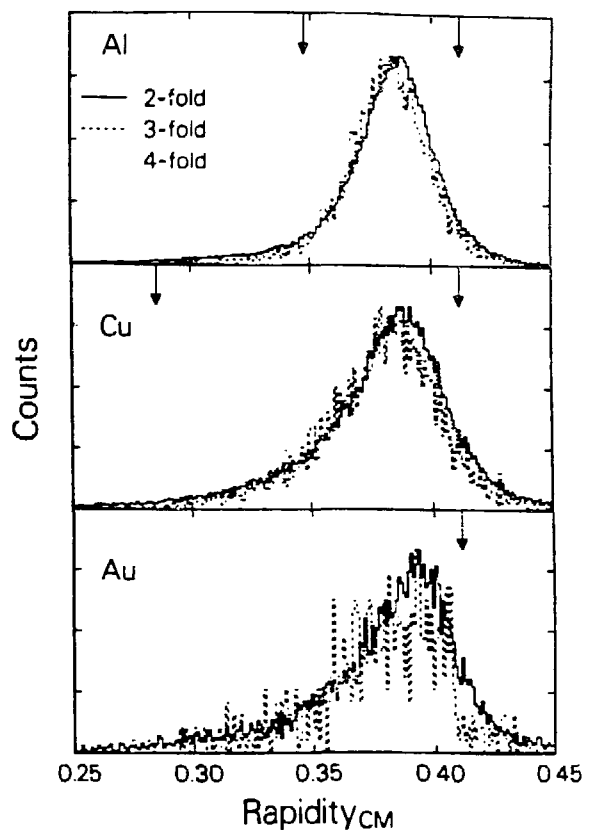


Fig. 11 Distributions of the center-of-mass rapidity for 2-fold, 3-fold, and 4-fold complex fragment ($Z>2$) events in the 80 MeV/u $^{139}\text{La} + ^{27}\text{Al}$, ^{nat}Cu and ^{197}Au reactions. The maxima of the distributions have been normalized to each other. The arrow at the larger rapidity in each subplot corresponds to the beam rapidity, the arrow at the smaller rapidity corresponds to the center-of-mass rapidity of the entrance channel.^{15/}

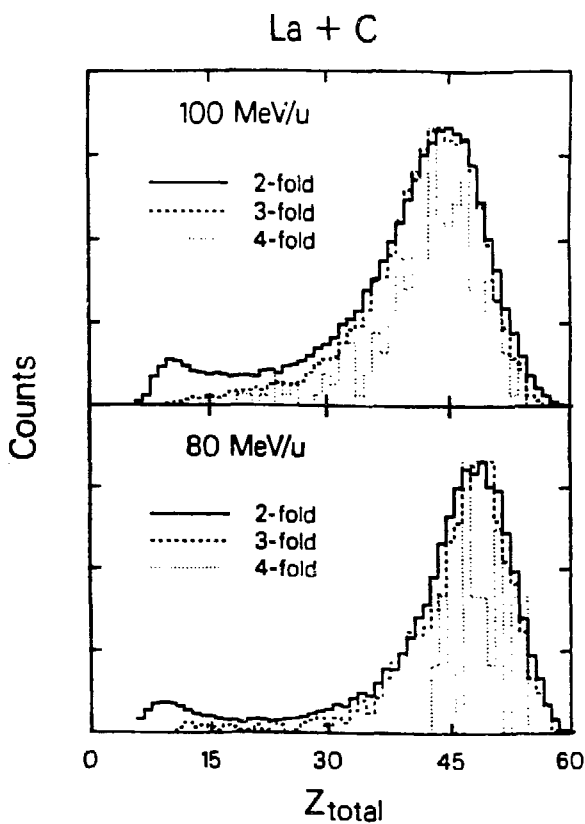


Fig. 12 Distributions of $Z_{\text{Total}}(Z_1 + Z_2)$ for 2-fold, 3-fold, and 4-fold complex fragment ($Z > 2$) events in the 80 and 100 MeV/u $^{139}\text{La} + ^{12}\text{C}$ reactions. The maxima of the distributions have been normalized to each other.^{15/}

As a point of philosophy, one may wonder whether one should approach the critical temperature from below or from above. It is our contention that the approach from below is by far more likely to succeed. We do not know what a nuclear system in thermodynamic equilibrium ought to look like just above the critical temperature. Furthermore, it is not obvious that standard reactions would produce it.

On the other hand, we know what nuclear systems look like below the critical temperature. In fact, we have produced these systems and followed their properties with ever increasing excitation energies. The knowledge of their standard decays, and, in particular, of their complex fragment decay, should allow us to detect the onset of critical instability as a departure from these lower temperature decay modes.

Is this multifragment decay a trivial extension of the binary decay, namely a series of sequential binary decays, or a new mode of compound nucleus decay not described heretofore, or, again, the manifestation of a general instability related to the vicinity of the critical temperature? These are, of course, fundamental questions whose answer can only come for a comprehensive study of these long lived intermediates.

Conclusion

The way to proceed in this study is fairly straight forward. First of all, it is necessary to follow in detail as a function of excitation energy the well known and characterized low energy decay. In particular, for the compound nucleus, the branching ratios between complex fragment emission and light particle emission must be understood quantitatively. This implies an understanding of the temperature dependence of the barriers leading to fission and to complex fragment emission. This knowledge will allow one to calculate the "expected sequential binary decay background" to multifragment emission, above which new processes may appear.

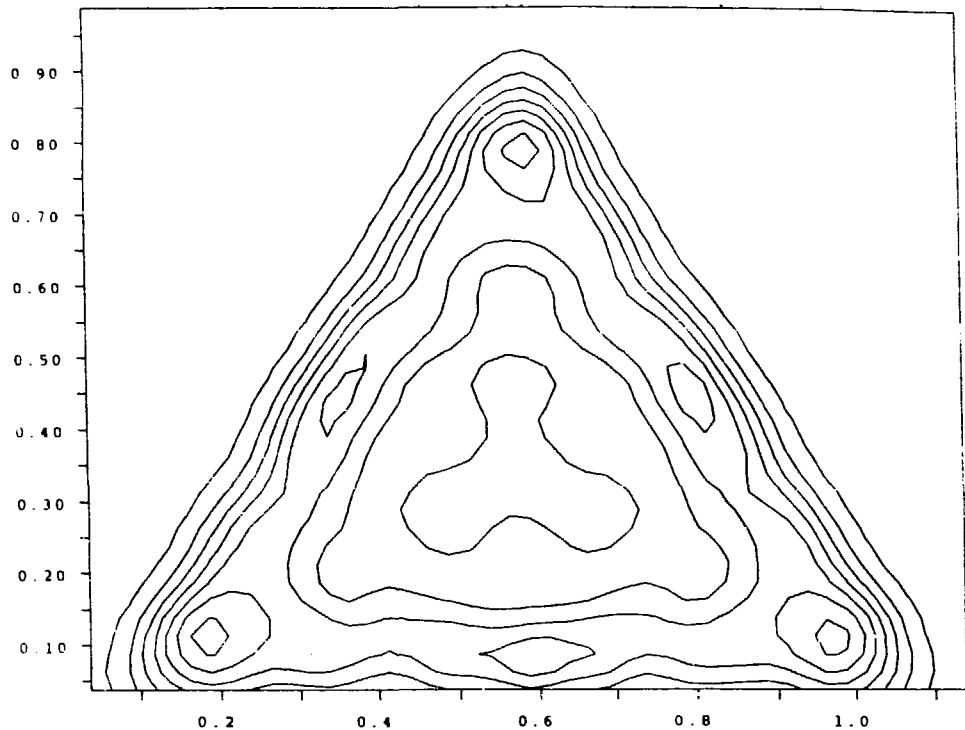


Fig. 13 Dalitz plot of 3-body events (Z_1 - Z_2 - Z_3) for the 80 A MeV $^{139}\text{La} + ^{12}\text{C}$ reaction./5/

References

1. M. Morjean et al., Phys. Lett., 1988, B203, p. 215.
2. L. G. Moretto and G. J. Wozniak, Prog. in Part. & Nucl. Phys., 1988, 21, p. 401.
3. R. J. Charity et al., Nucl. Phys., 1988, A483, p. 371.
4. N. Colonna et al., Phys. Rev. Lett., 1989, 62 p. 1833.
5. D. R. Bowman, Ph. D. thesis, 1989, Lawrence Berkeley Laboratory preprint No., LBL-27691.
6. L. G. Moretto and D. R. Bowman, Proc. of the XXIV Int'l Winter Meeting on, Nucl. Phys., 1986, Bormio, Italy, Jan. 20 - 25, 1986, Ricera Scientifica ed Educazione Permanente, Suppl., N. 49, p. 126.
7. L. G. Sobotka et al., Phys. Rev. Lett., 1983, 52, p. 2187.
8. M. A. McMahan et. al., Phys. Rev. Lett., 1985, 54, p. 1995.
9. R. J. Charity et. al., Nucl. Phys., 1989, in press, LBL-26859.